

## Astronomical performance of the engineering model Ørsted Advanced Stellar Compass

Allan Eisenman<sup>†</sup>  
Carl Christian Liebe<sup>\*</sup>  
John Leif Jørgensen<sup>\*</sup>

<sup>†</sup>Jet Propulsion Laboratory  
California Institute of Technology  
4800 Oak Grove Drive, Pasadena, CA 91109

<sup>\*</sup>Technical University of Denmark  
2800 Lyngby, Denmark

### ABSTRACT

The Danish geomagnetic microsatellite, Ørsted, is an autonomous spacecraft which is scheduled for a May 1997 launch into polar orbit. It is produced by a consortium of universities, industry and government and is Denmark's first national spacecraft. NASA support includes JPL real sky evaluation of its star tracker, the Advanced Stellar Compass (ASC).

The ASC features low cost, low mass, low power, low magnetic disturbance, autonomous operation, a high level of functionality and the high precision. These features are enabled by the use of advanced optical and electronic design which permit the direct integration of the ASC and the science payload. The ASC provides the required attitude information for its associated vector magnetometer and the spacecraft. It consists of two units, a CCD based camera head and a data processing unit with a powerful microcomputer. The microcomputer contains two large star data bases which enable the computer to recognize star patterns in the field-of-view, to quickly solve the lost-in-space acquisition problem and to derive the attitude of the ASC camera head.

The flight model of the camera head has a mass and a power consumption of 127 grams (without baffle) and 0.5 W, respectively. Typical, beginning-of-life, relative measurement precisions in pitch and yaw are in the order of two arcseconds (1  $\sigma$ ) or better have been achieved in the tests and are substantiated.

**Key Words:** Autonomy, Advanced Stellar Compass, CCD imaging, spacecraft star trackers, Ørsted mission

### 1.0 INTRODUCTION

The Ørsted spacecraft is Denmark's first national spacecraft. It is a microsatellite designed for a polar orbiting geomagnetic mission. Launch is scheduled for May 1997. The Ørsted project is being undertaken by a Danish consortium of Universities, Industry and Government. It will be the first precision mapping of the Earth's magnetic field since the NASA Magsat satellite flew in the late 1970s.

Support for the Ørsted mission is international. CNES of France is supplying a scalar magnetometer. DLR of Germany is supplying environmental testing and magnetic calibration. The US space agency, NASA, is supplying the mission with launch services, a JPL TurboRogue Global Position System receiver (GPS), science data reduction, analysis, and interpretation, and JPL evaluation and review of the Advanced Stellar Compass (ASC) star tracker.

The ASC is mounted on a boom 6m from the spacecraft body. The ASC provides precision attitude reference for the vector magnetometer. Reduced precision attitude reference information is supplied for the attitude control of the spacecraft. The ASC is a second generation class of CCD star tracker, incorporating full autonomy, including, an internal solution of the lost in space problem.

The ASC is housed in two assemblies, the Camera Head Unit (CHU) and the Data Processing Unit (DPU)<sup>2</sup>. The engineering model (EM) of the CHU is shown in Figure 1. The EM differs from the flight model in its use of an aluminum electronics case, a brass lens barrel and a planar mount.

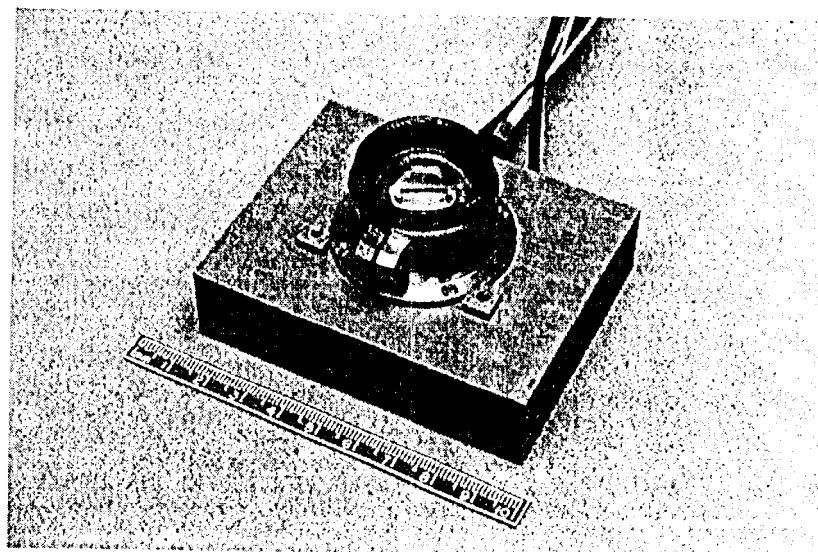


Figure 1, The EM CHU

The CHU uses a Sony CDX039AI CCD and its associated driver IC set. The CCD has 752x582 pixels each with an effective dimension of  $8.6\mu\text{m} \times 8.3\mu\text{m}$ . The CCD is an interline, interlaced CCD with a micro lens for improved fill factor and sensitivity. The CHU lens is custom designed for this star tracker and its point spread function is optimized to cover multiple pixels with a minimum amount of defocusing, resulting in improved stability over a wide range of temperatures. The ASC is designed and tested to operate in space with a total dosage of up to 10 KRad.

Key parameters for the Ørsted flight model ASC are listed in Table 1.

Table 1. ASC key parameters

Parameter	Value
NEA*	
Pitch/Yaw	$\sim 1$ arcsec. $1\sigma$
Roll	$\sim 6$ arcsec. $1\sigma$
Relative accuracy*	
Pitch/Yaw	$\sim 2$ arcsec. $1\sigma$
Roll	$\sim 16$ arcsec. $1\sigma$
Magnitude error*	0.13 m, $1\sigma$
CHU/DPU	
Mass	127/1400 g
Power consumption	0.5/5 Watts
Field of view	$16^\circ \times 22^\circ$
Update rate	0.9 Hz
Stars tracked	25 min., 200 max., 65 typ.
Sensitivity	6 m
CHU residual magnetization	$\sim 1$ nT

\* As measured at TMO with EM CHU

A block diagram of the ASC is shown in Figure 2. The CHU generates an analog video signal which is digitized and stored by the framegrabber in the DPU. The image can be read either by the CPU (in normal mode) or by an external device (in the emergency bypass mode). The CPU calculates the attitude based on the image and the star catalog, stored in a 11Mbit code protected memory. All communications are routed through the telemetry interface in fully packetized form.

The flight processor is a 50-MHz Intel 80486 processor running at 20 MHz. The program, data and status parameters are downloaded from a Hamming code protected (2 bits detection, 1 bit correction) 2-Mbytes flashram to the 4-Mbytes DRAM.

The DPU is equipped with multiple protection mechanisms. All major chips are individually protected against latchup by power shutdown which is triggered by over current. The ASC is also equipped with a woodpecker. This is an RC circuit connected to the reset line. A special command needs to be issued at regular intervals, or the ASC will be met. The inherent protection mechanism "protected mode" in the 486 architecture is also fully utilized to detect and trap errors. The ASC has a police program that will reset the ASC if an operation stops. The ASC bitwashes the hamming coded memory at regular intervals. All programs, data and system settings (except for a small bootstrap in Rad hard fuse linked PROM) can be uploaded during flight.

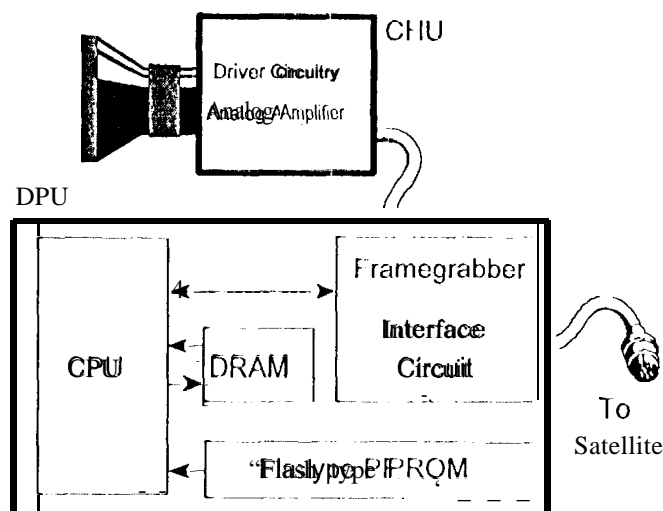


Figure 2. Block diagram of the ASC

After the DPU gains access to the digitized image it analyzes the star positions in order to calculate the pointing direction of the boresight and the roll angle around it. The actual image processing applied to the image depends on several conditions.

In normal operation the angular difference between two consecutive images is small enough to enable, first, sifting the image for stars, then, deriving star centroids, and finally, applying corrections. Based on the previous attitude quaternion and the star catalog, an artificial star image is created. Then a spherical, least squares fit between the images is performed. Finally, astronomical corrections (precession, nutation, light time aberration) are applied to the attitude quaternion.

In a number of situations, e.g., after power cycling or after SEUs (single event upsets), the previous attitude is inadequate or missing. In this case an additional image processing step is included, the initial attitude acquisition. The initial attitude acquisition is a pattern recognition of the stars in the FOV and it is done by measuring the distance to the first and second neighboring stars and the angle between them, creating a 'triplet.' All conceivable triplets on the celestial sphere from the brighter stars are included in the star database<sup>3</sup>. A fast and robust solution is achieved by matching the measured triplets against the internal database.

## 2.0 THE EVALUATION AT TABLE MOUNTAIN OBSERVATORY

The EMASC was evaluated at the JPL operated facility at "Table Mountain observatory, CA (TMO) on December 9, 10 and 11, 1995 when its CIU was mounted on a 24 inch telescope. No observations were made through the telescope, it only served as a pointing mount for the CHU. The CHU was mounted on the front of the telescope. The two instruments were only coarsely aligned relative to each other. Therefore, the angle between their respective boresights was estimated to be as large as 2° or 3°. Figure 3 shows the EMCHU mounted on the front of the telescope.

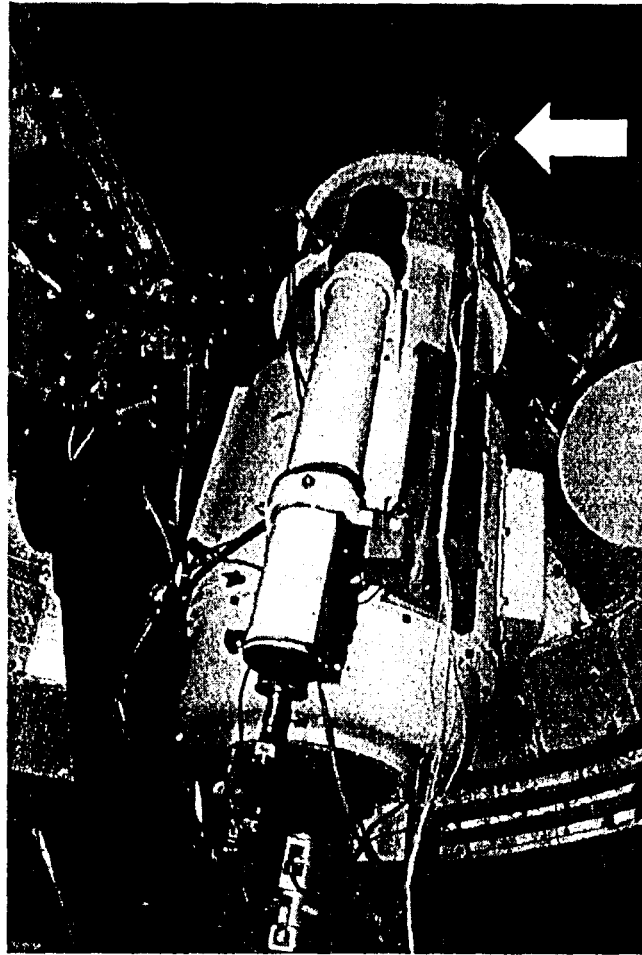


Figure 3. EMCHU mounted on the 24 inch telescope

During the evaluation program, two series of measurements were acquired. The first series was taken with the telescope tracking specific celestial coordinates. It was used to derive the NEA (Noise Equivalent Angle) of the ASC. The second series was acquired with the telescope pointing towards zenith. It was used to derive the relative accuracy of the ASC. The images were acquired with a DOS based personal computer using a Pentium processor and a framegrabber instead of the actual flight DPU. This was done because it was desired to store all of the frames on the computer hard disc to enable later changes in the data reduction. The flight system uses precision time from a GPS receiver in the reduction of each frame to calculate the light time aberration as well as time stamping. Since no GPS receiver was used with the EM system, the time that each frame was acquired was only known to within approximately one second. This limited the system pointing, knowledge and the ultimate EM accuracy. The images in this PC based EM system were separated by approximately 4 seconds (mainly limited by the speed of the PC data storage).

### 3.0 VARIATION OF THE ATTITUDE ESTIMATE, FIRST DATA SERIES

1 During the first series the telescope was commanded to track the celestial sphere at coordinates of  $\delta = 34.24^\circ$ ,  $\alpha = 3h11m$ , starting at zenith. This series includes 572 images. During the series, the celestial coordinates of the attitude were constant, and consequently the tracked star fields were approximately constant. The image frames can be used to determine the NEA of the system, and obtain statistics of the individual star positions. Figure 4 through 6 show the declination, right ascension and roll angle outputs of the ASC for all of the frames acquired in the series.

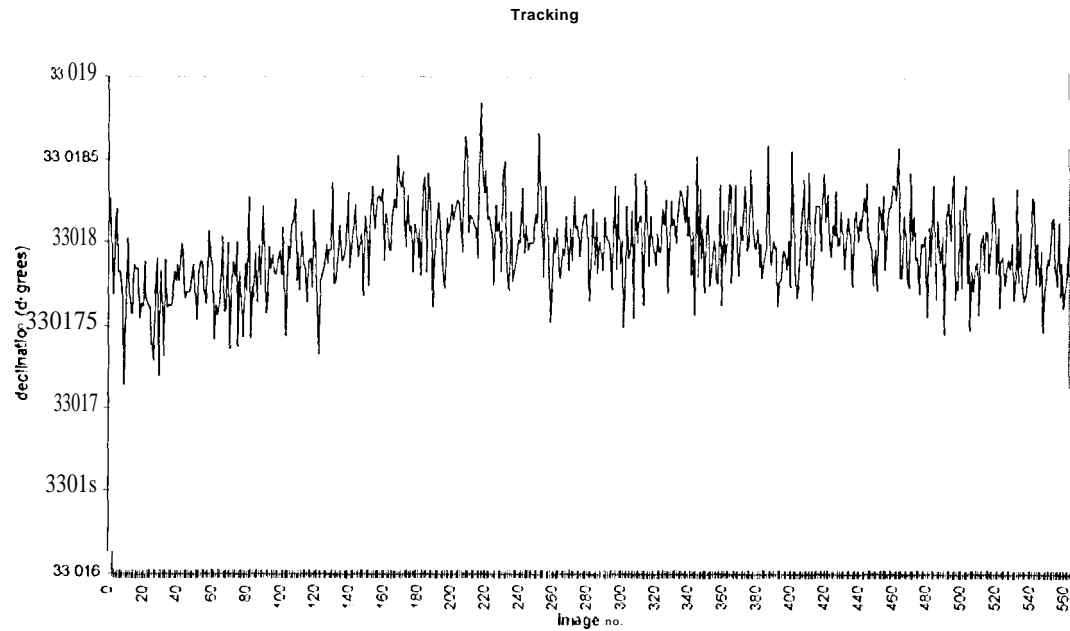


Figure 4. Declination during tracking

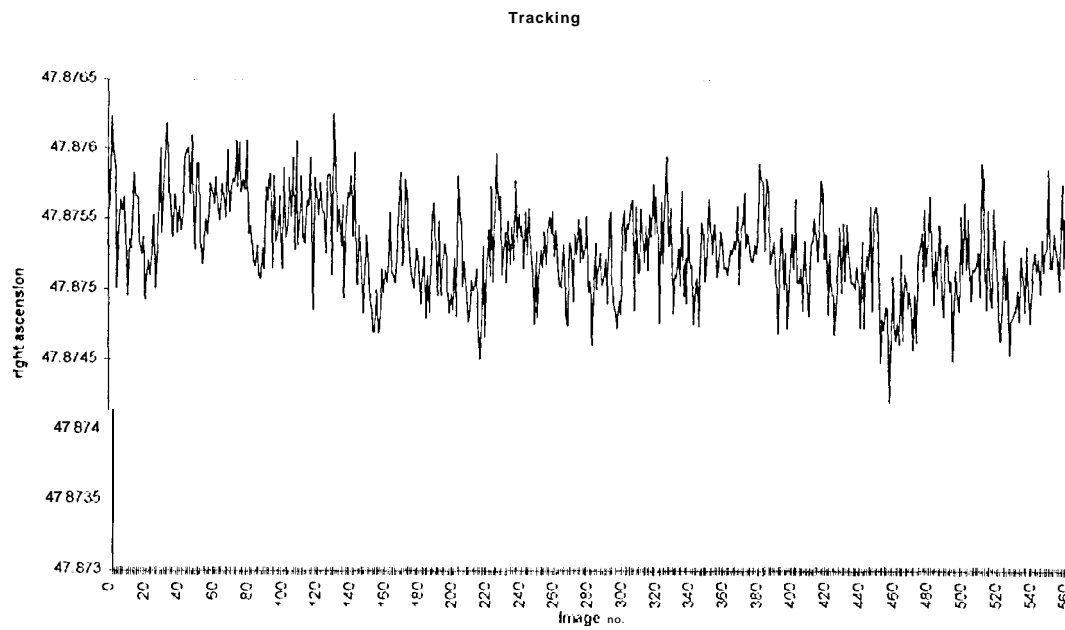


Figure 5. Right ascension during tracking,

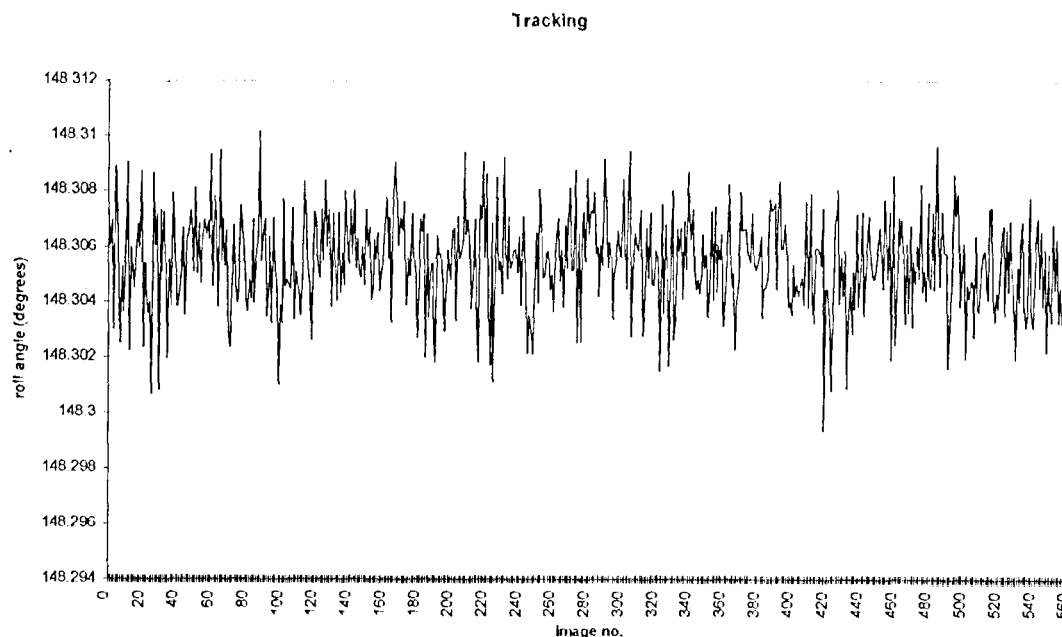


Figure 6. Roll angle about CHU boresight during tracking

A statistical analysis of the variation of the attitude angles was done by assuming that the mean values of the angles were constant. A Gaussian distribution was assumed. The results are given in Table 2.

Table 2. NFAs in celestial coordinates

	1 $\sigma$ (68.3% within)	2 $\sigma$ (95.4% within)	3 $\sigma$ (99.7% within)	rms
Declination:	0.9''	1.7''	2.6''	0.9''
Right ascension:	1.3''	2.4''	3.2''	1.2''
Roll angle:	6.0''	12.1''	16.1''	6.2''

ASC referenced pitch and yaw NFAs were derived by a geometric transformation of the celestial referenced NFA's as depicted graphically by the ellipse in Figure 7.

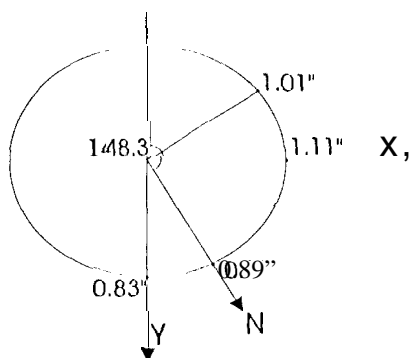


Figure 7. Relationship of NFA in celestial coordinates to NFA in instrument coordinates

The resulting values are given in Table 3.

Table 3. Pitch and yaw values of NEA

	pitch	yaw
rms	1.1''	0.8''

It is observed that the NEA is not equal in yaw and pitch. The explanation for this is threefold. First of all, the CIU was mounted on a telescope that was tracking. The telescope was equatorial mounted, i.e. it mainly used one motor to track the sidereal rate. Hence, telescope motor noise is primarily added in the right ascension direction. Next, the CIU is operating in interlaced mode. This implies that the algorithm deriving the centroids is operating differently in yaw and pitch, resulting in different performance in yaw and pitch. Finally, the angular resolution is not the same in yaw and pitch.

It should be noted that in Figure 4- Figure 6 there is a drift. This is most likely an artifact of the data taking, including atmospheric effects. This artifact makes the measured NEA larger than that of the ASC itself.

#### 4.0 RELATIVE ACCURACY, SECOND IMAGE SERIES

The second series of 342 images was taken with the telescope pointing at zenith. Zenith was chosen because the perturbation of the airmass was the smallest here. By examining the variation of the declination and roll angle, or the rate of change of the right ascension, it is possible to determine the relative accuracy, because the FOV of the ASC is drifting across the celestial sphere at the sidereal rate. The effects of systematic errors, due to changing star fields, are included in the variations as the ASC locks on to different constellations of stars.

When looking at zenith, the declination remains constant, while the right ascension drifts with the sidereal rate, assuming the epoch and equinox of the star catalog in the ASC are equal to the current time (December 10, 1995, 6:15 GMT). It should be noted that the effect of the airmass of modifying the FOV is inherently included in the calibration, as it is made through the atmosphere.

The output from the ASC during the zenith series is shown in Figure 8 and Figure 9. Figure 8 displays the declination output. Figure 9 displays the roll angle. While the flight ASC uses precise GPS time and date, the FM does not, and only utilizes the PC time with a resolution of one second. As the celestial sphere drifts across the FOV with the sidereal rate in the right ascension, it is not possible to reconstruct this value, as one second corresponds to 15 arcsec. and consequently will dominate the measurements.

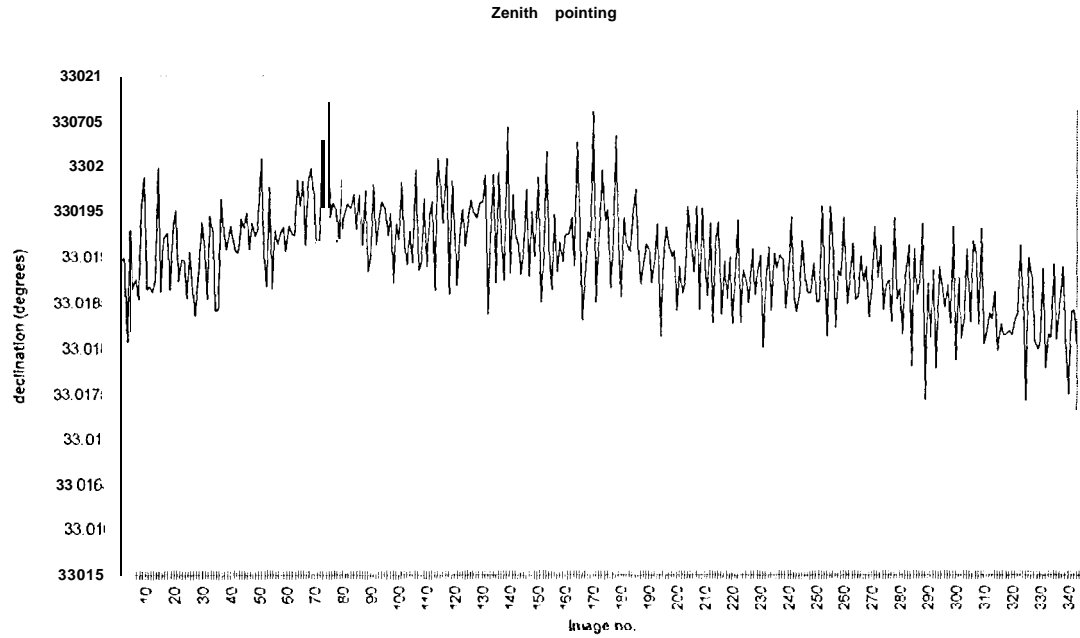


Figure 8. Declination during zenith pointing

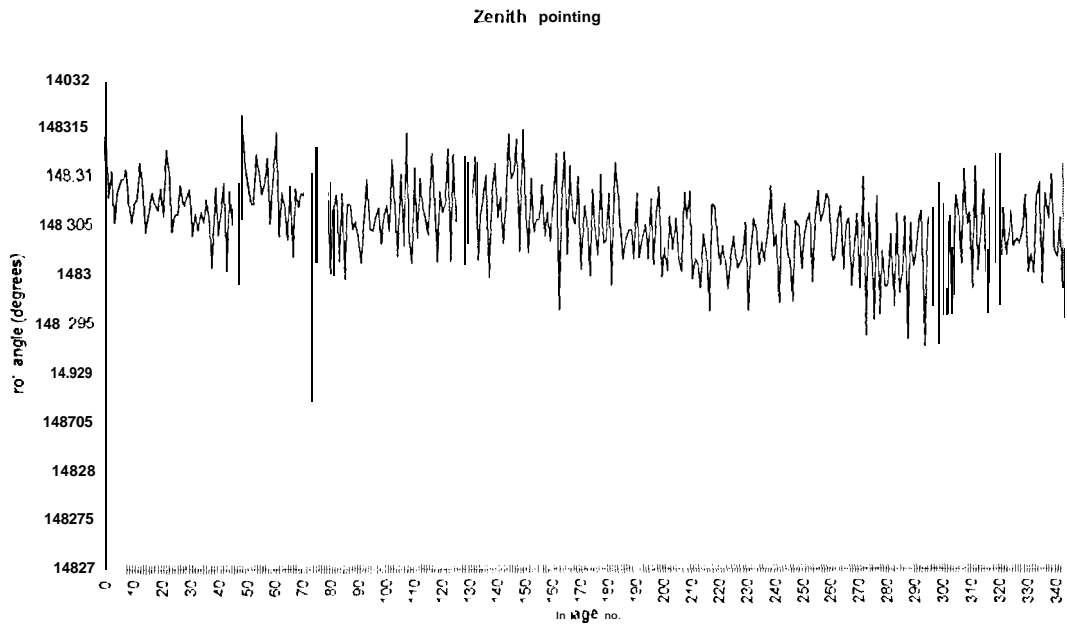


Figure 9. Roll during zenith pointing

A statistical analysis of the variations of the angles was done by assuming that the means of the angles were constant. A Gaussian distribution was assumed. The results are given in Table 4.



Table 4. Relative accuracy

	1 $\sigma$ (68.3% within)	2 $\sigma$ (95.4% within)	3 $\sigma$ (99.7% within)	rms
Declination:	1.9''	3.8''	5.7''	2.0''
Roll:	15.1''	30.9''	43.5''	16.0''

While NEA has several components including terms with relatively high temporal frequencies, it does not include errors caused by changing star patterns, nor calibration error terms. The error terms which are caused by changing star patterns can be measured by the zenith pointing, second data series, with its inherent varying star fields.

If the lens correction function, the centroiding, the star catalog etc. were ideal, the NEA of the tracking and zenith series would be the same. However, there will always be correction residuals so that the relative error of the zenith series will be higher than the NEA of the tracking series. This is confirmed by the measurements of about one arcsec and two arcsec, for NEA and relative accuracy respectively (both 1 axis, 1  $\sigma$ ).

It should be noted that NEA and relative accuracy are terms in the larger error budget. They are both referenced to the CCD image itself. The absolute accuracy is referenced to the ASC CHU mounting interface which is the reference for the spacecraft and its payload. Many mechanical paths relate these terms to the CHU mounting. The CCD and lens move relative to the reference. These shifts in position are caused by mounting uncertainty, launch loads, gravity release, temperature changes, etc. The CHU minimizes the mounting uncertainty term by employing a precision three ball bearing, kinematics mount. Other terms in the error budget include calibration, or knowledge terms. In sum, the absolute attitude error of the boresight pointing is estimated to be a few arcsec higher than the measured relative accuracy.

#### 5.0 NEA OF INDIVIDUAL STARS IN THE TRACKING SERIES

To further analyze, and if possible, to decompose the relative position error, we chose to measure the relative precision of each of the individual stars.

The tracking series includes 572 images of the same star scene. The average number of stars in each image is 50.1 and 45 of them are detected in **500** frames or more. The number varies due to occasional satellite over fly and dim stars dropping below the detection threshold. Figure 10 shows a typical image from the series.

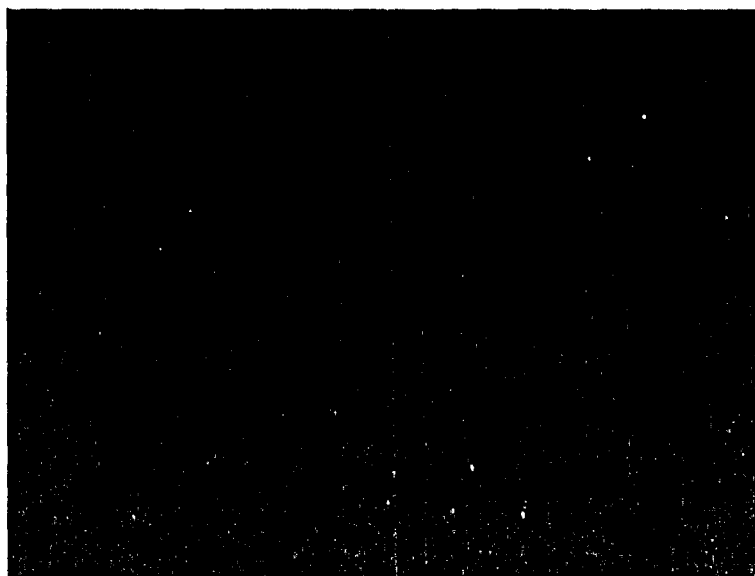


Figure 10. Typical tracking series image frame

The spatial position variation of the 45 individual stars was calculated for the more than **500** images in which they were included. The mean position and the position RMS variance from the mean were calculated, assuming a fixed position for each star. The averages of the spatial variations are displayed in Table 5.

Table 5. Position variations of individual stars

	rms x	rms y	rms total
Single star:	3.0''	3.8''	4.9''

## 6.0 POSITION RESIDUAL OF INDIVIDUAL STARS IN THE ZENITH POINTING SERIES

The NEA of a star position is an important component of the error budget. However, the error between the star position and the star catalog position is usually much larger, because it includes lens distortion, centroiding effects, CCD position shift etc. This larger error we define as the "star position residual". Figure 11 shows an artificial least squares fit<sup>4</sup> between a synthetic star image and a star catalog frame. Solid circles represent the star catalog and the white circles the measured stars.

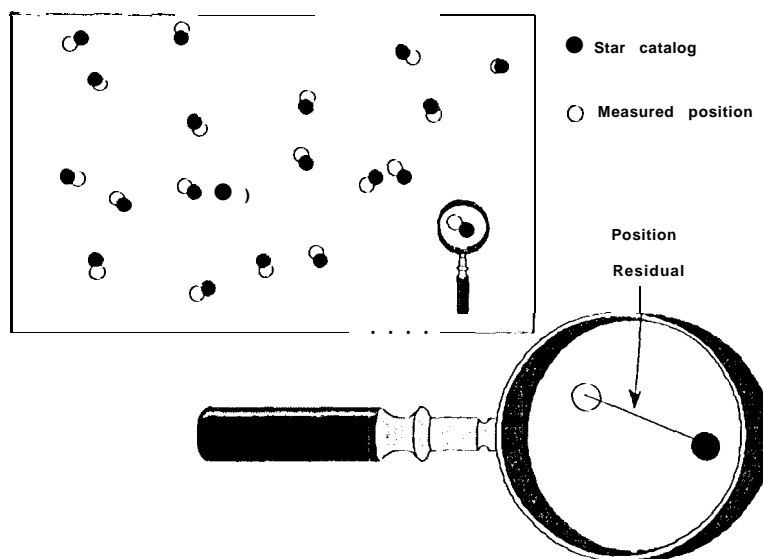


Figure 11. Graphical illustration of the position residual

As, expected, these residuals varies from star to star and from image to image. in Figure 12 and Figure 13, the probability distributions of the residuals in pitch and yaw for all stars in all images in the zenith series as shown:

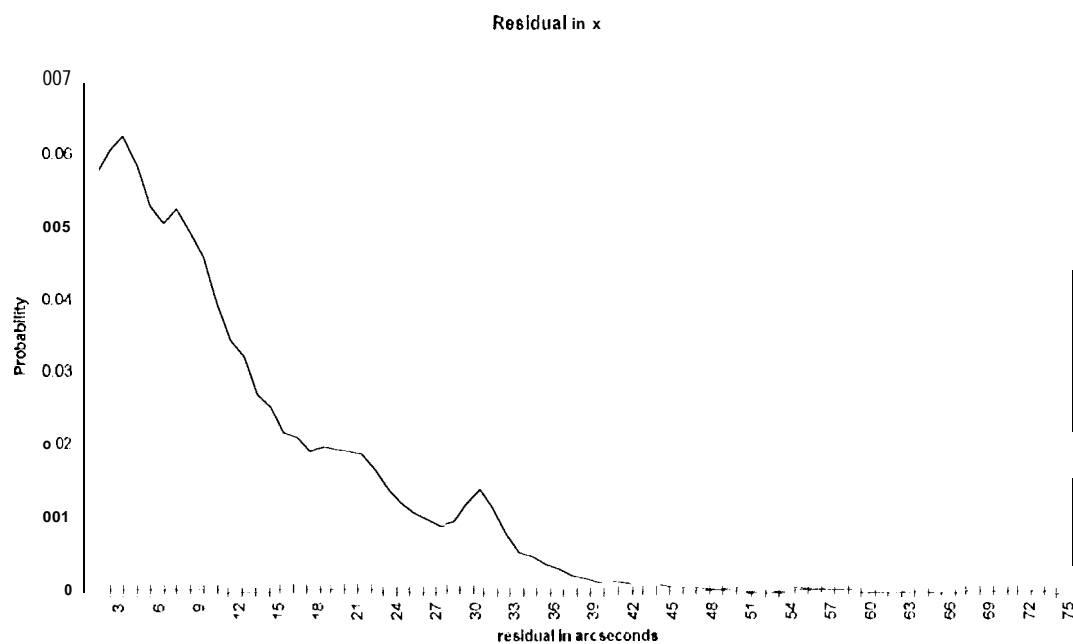


Figure 12. Residual in pitch

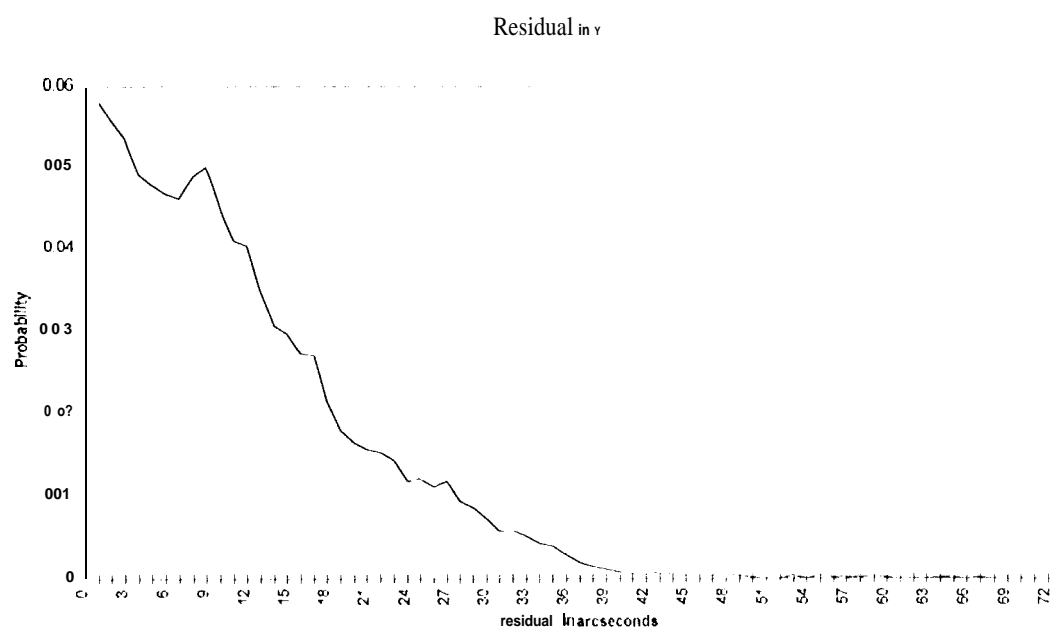


Figure 13. Residual in yaw

The  $\sigma$ 's and rms are given in Table 6.

Table 6. Star position residuals

	1 $\sigma$ (68.3% within)	2 $\sigma$ (95.4% within)	3 $\sigma$ (99.7% within)	rms
pitch	14.3''	31.8''	56.0''	15.6''
yaw	13.6''	29.4''	64.3''	15.2''

It is observed, that the position residual of a star is approximately 15 arcseconds. This should be compared to the N/A of approximately 3.5 arcseconds. This indicates the level of true noise and systematic errors in the ASC.

## 7.0 MAGNITUDE STABILITY

A significant property of the ASC is its ability to determine the brightness of a star and the stability of that value, even though these are only used for thresholding in the initial attitude acquisition and tracking algorithm.

The star brightness is determined by summing the net pixel intensity values (those above the background level), in the close vicinity of a star. The variation in star brightness is determined from its net total value change over multiple frames. The zenith series was used to include the effects of uneven light sensitivity across individual CCD pixels, as this effect will be evident as a star image moves across a pixel at the sidereal rate. The variation in intensity for a typical star is shown in Figure 14.

For the typical star in Figure 14, the brightness variation is 1 S. 1% RMS. A total number of 346 frames was used. The average number of stars per frame remained at 50.1 with 45 of these appearing in more than 250 frames. The resulting average RMS brightness variation (b) is derived from the 45 stars:

$$b = 13.4\% = 2.5^{0.134} = 0.13 \text{ mag}$$

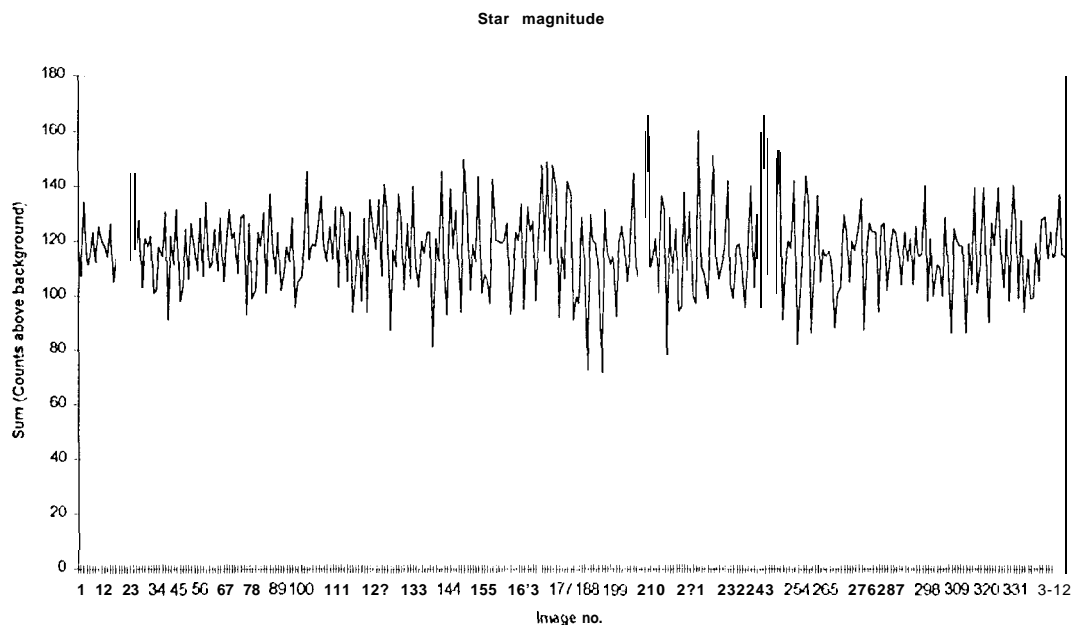


Figure 14. Star magnitude variation

## 8.0 CONCLUSION

The accuracy of a star tracker is an essential parameter. Since the accuracy of a star tracker can be measured and specified in a variety of ways, it is difficult to compare the performance of different star trackers. The principal objective here has been twofold: 1) to evaluate the N/A and relative accuracy of the engineering model of the ASC for the Ch-stel sciencecraft, and 2) to describe how these are defined and measured using the real sky.

The ASC was evaluated utilizing two series of real sky images obtained at the JPL, "Table Mountain Observatory. The first series was taken while tracking the celestial sphere, and the second series while pointing at zenith. The tracking series yielded NEA values of 1.1 arcsec in pitch, 0.8 arcsec in yaw, and 6.2 arcsec in roll, all RMS. The zenith series, measuring the relative accuracy, yielded approximately double these values in pitch and yaw, and 16 arcsec, 1 MS, in roll.

The spatial position variations of single stars were deduced from the tracking series. The average values were 3.8 arcsec in pitch, and 3 arcsec in yaw, RMS. The average value of the position residual error of individual stars was found to be approximately 15 arcsec RMS in both axes.

In conclusion, the accuracy of the ASC is generally better than most conventional, commercial star trackers. This accuracy has not previously been combined with autonomous, initial attitude acquisition capability nor such low mass and power-. This real sky evaluation of the ASC has cemented the advantages of simultaneously tracking multiple stars (>25).

## 9.0 ACKNOWLEDGMENT

This work has been sponsored by: NASA code YSG, the Technical University of Denmark, the Ørsted project and the Radioparts Foundation.

## 10.0 REFERENCES

1. The Ørsted Project, Pamphlet, Computer Resources International, Birkerød, Denmark, 1994.
2. Eisenman, A.R.; Jørgensen, J. I.; Liebe, C.C: Real Sky Performance of the Prototype Ørsted Advanced Stellar Compass, IEEE Aerospace Application, Snowmass, CO, Feb. 1996.
3. Liebe, C.C: Star Trackers for Attitude Determination, IEEE Aerospace and Electronics Magazine, June 1995, p. 10-16.
4. Shuster, M.D; Oh, S.D: Three-Axis Attitude Determination from Vector Observations, Journal of Guidance, Control and Dynamics, Volume 4, number 1, p.70-77.